



Contents lists available at ScienceDirect



Catalysis Today

journal homepage: www.elsevier.com/locate/cattod

Propylene glycol oxidation with *tert*-butyl hydroperoxide over Cr-containing metal-organic frameworks MIL-101 and MIL-100

Viktoria V. Torbina^a, Irina D. Ivanchikova^{a,b}, Oxana A. Kholdeeva^{a,b}, Igor Y. Skobelev^b, Olga V. Vodyankina^{a,*}

^a Tomsk State University, Lenin Ave. 36, Tomsk 634050, Russia

^b Borekov Institute of Catalysis, Lavrentiev Ave. 5, Novosibirsk 630090, Russia

ARTICLE INFO

Article history:

Received 28 December 2015

Received in revised form 12 April 2016

Accepted 15 April 2016

Available online xxxx

Keywords:

Propylene glycol

Selective oxidation

Hydroxyacetone

Metal-organic frameworks

tert-Butyl hydroperoxide

ABSTRACT

Chromium-based metal-organic frameworks MIL-101 and MIL-100 catalyzed oxidation of propylene glycol (PG) using *tert*-butyl hydroperoxide (TBHP) as oxidant. The main oxidation product was hydroxyacetone (HA) while minor oxidation products were acetaldehyde and acetic acid. The best results (88% selectivity toward HA at ca. 10% PG conversion) were achieved over MIL-101 using acetonitrile as solvent. In water, C–C bond cleavage products predominated. MIL-101 and MIL-100 revealed different behavior toward adsorption of PG from MeCN solution, which affected their catalytic performances. Additives of radical chain scavengers produced a strong rate-inhibiting effect whereas the presence of molecular oxygen accelerated the reaction, suggesting radical chain mechanism of the oxidation process. The oxidation of PG over MIL-101 at 50 °C proceeded without leaching of the active metal into solution and the catalysis had the truly heterogeneous nature. The MIL-101 catalyst could be recycled without significant loss of activity and selectivity and preserved its structure during, at least three, catalytic cycles.

© 2016 Elsevier B.V. All rights reserved.

1. Introduction

The selective oxidation of alcohols and diols to carbonyl compounds plays a key role in organic synthesis [1]. Traditional methods for such transformations involve the use of stoichiometric inorganic oxidants, notably, chromium(VI) reagents [2,3]. In the past decades, a range of homogeneous catalyst systems have been developed for the selective oxidation of OH functional groups [4]. However, from both economic and environmental viewpoints, there is a growing demand for atom efficient catalytic methods employing environmentally benign oxidants and truly heterogeneous catalysts that can be easily recovered and recycled [5,6].

Conversion of bio-renewable feedstocks to valuable products remains a formidable challenge [7]. Propylene glycol (PG) is one of base chemicals that is traditionally produced from propylene oxide but can also be generated from glycerol, a low-cost by-product in transesterification of triglycerides for biodiesel production [8]. A number of value-added products, such as hydroxyacetone (HA, also called acetol), methylglyoxal, lactic acid and pyruvic acid, which

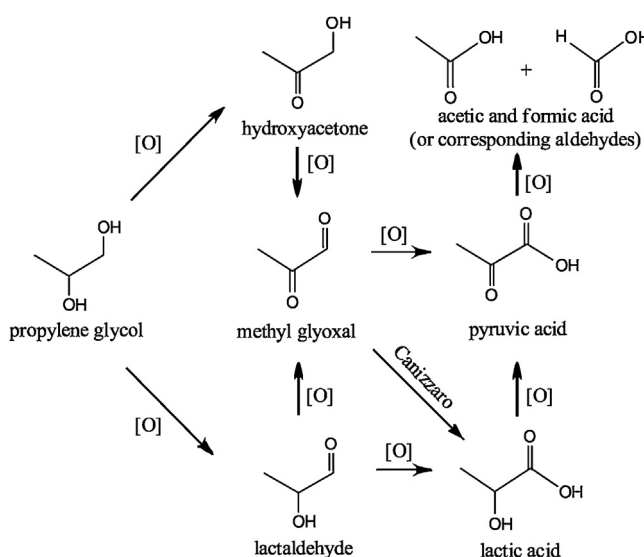
find application in the production of fine chemicals and pharmaceuticals, can be obtained through oxidation of PG (**Scheme 1**).

PG oxidation in the gas phase over iron phosphate catalysts afforded methyl glyoxal as the main product [9,10]. Vapor phase dehydrogenation of vicinal diols, including PG, to produce α-hydroxyketones was accomplished using various copper catalysts [11]. PG reacted with molecular oxygen to form HA as the initial product and methylglyoxal via subsequent oxidation of HA on Ag catalysts (500–700 K) [12,13]. The majority of publications on PG oxidation in the liquid phase have been devoted to the production of lactic acid using Pd-, Pt- and Au-containing catalysts in alkaline conditions [14–18]. Very few works reported liquid-phase selective oxidation of PG to HA, pointing out that this reaction is accompanied by C–C bond cleavage processes, which decreases selectivity toward acetol [19,20]. In particular, Sheldon and Dakka oxidized PG to HA using H₂O₂ as oxidant and titanium-silicalite TS-1 as heterogeneous catalyst [19]. Kholdeeva et al. have demonstrated that this reaction can be accomplished with H₂O₂ using a Ti-containing sandwich type polyoxometalate as homogeneous catalyst [20].

Although HA is used in medicine, food, textile, cosmetic and polymer industries, the scope of its application is still limited by its high cost [21]. The reason for that is employment of non-catalytic multistep technologies that deliver HA with poor selectivity and require expansive purifying steps. Therefore, the development of

* Corresponding author.

E-mail address: vodyankina.o@mail.ru (O.V. Vodyankina).



Scheme 1. Oxidative transformations of PG.

effective catalytic systems for the selective oxidation of PG to HA using environmentally friendly oxidants and easily recyclable heterogeneous catalysts remains a demanding task.

Metal-organic frameworks (MOFs), a new emerging class of crystalline materials that consist of coordination bonds between nodes of metal ions and multidentate organic linkers, have attracted much recent attention as functional materials for adsorption, gas separation and storage techniques, as well as heterogeneous catalysis [22–26]. MOFs possess a unique combination of properties that includes extremely high surface areas and pore volumes, tunable pore size and functionalities, and large fraction of uniform and accessible metal sites. However, relatively low thermal and hydrothermal stability may constrain their practical applications, in particular, in gas-phase heterogeneous catalysis [25,27].

Férey et al. reported the synthesis of mesoporous chromium-based carboxylates MIL-101 ($[Cr_3X(H_2O)_2O(BDC)_3]$; X=F, OH; BDC=1,4-benzenedicarboxylate; MIL stands for Materiaux de l'Institut Lavoisier) [28] and MIL-100 ($[Cr_3X(H_2O)_3O(BTC)_2]$; X=F, OH; BTC=1,3,5-benzenetricarboxylate) [29], which demonstrated good resistance to air, water, common solvents and thermal treatment (up to 275 °C in air). Both MIL-101 and MIL-100 consist of quasi-spherical mesoporous cages of two types (34 and 29 Å in MIL-101 versus 29 and 25 Å in MIL-100) which are accessible through microporous windows (16 and 12 Å in MIL-101 versus 8.6 and 5.5 Å in MIL-100). The amount of Cr is 23 and 26 wt.% in MIL-101 and MIL-100, respectively. Coordinatively unsaturated metal sites (CUS) can be easily created in the structure of these MOFs by heating in vacuum [30]. All these make MIL-100 and, especially, larger pore MIL-101 attractive candidates for catalysis in the liquid phase [31,32]. In particular, selective oxidations of cyclohexane [33] and a range of unsaturated hydrocarbons [34–38] could be accomplished using *tert*-butyl hydroperoxide (TBHP) and/or molecular oxygen as oxidant.

The aim of this work was to explore the potential of the chromium-based MOFs, MIL-101 and MIL-100, for the selective oxidation of PG. The effects of the oxidant nature and reaction conditions (temperature, concentrations of reagents, solvent nature, and atmosphere) on the product selectivity and yield have been investigated. Special attention was paid to determine the nature of catalysis and evaluate catalyst reusability.

2. Experimental

2.1. Materials

Propylene glycol (Component-reactiv, 99%) and ethyl acetate (Himabsolut, 98%) were distilled under vacuum and atmospheric pressure, respectively. Other reagents were purchased from Sigma Aldrich and used without further purification. All organic solvents were dried and stored over activated 4 A molecular sieves. TBHP was used either as a 5.5 M solution in decane or as a 70 wt% solution in water. The concentration of active oxygen before and after catalytic reactions was determined by iodometric titration.

2.2. Catalysts preparation and characterization

Cr-MIL-101 was synthesized by the solvothermal method following the procedure of Férey et al. [28] with some modifications reported elsewhere [36]. Synthesis of Cr-MIL-100 was performed according to the literature [29] following the protocol described previously [37]. Activation of MOFs was carried out in vacuum at 150 °C for 5 h and then at 180 °C for 2 h.

Textural characteristics of the catalysts were determined from nitrogen adsorption isotherms (77 K; Sorbtometr M instrument). Before measurements the samples were degassed at 180 °C under vacuum during 6 h. MIL-101 and MIL-100 revealed BET surface area of 3100 and 2100 m² g⁻¹ and pore volume of 2.1 and 0.9 cm³ g⁻¹, respectively. The structure of the MIL-101 and MIL-100 materials was confirmed by XRD (Philips APD1700 X-ray diffractometer). XRD patterns of the samples of Cr-MIL-100 and Cr-MIL-101 versus simulated X-ray patterns of these MOFs are shown in Fig. S1 in Supporting Information (SI). The preservation of the MOF structure was also verified by FT-IR spectroscopy (SCIMITAR FTS 2000 spectrometer). Corresponding FT-IR spectra are given in Fig. S2.

2.3. Catalytic experiments and product analysis

Catalytic oxidation tests were carried out in a temperature-controlled glass vessel at 40–70 °C under vigorous stirring (500 rpm). Typically, the reaction was initiated by the addition of TBHP to a mixture containing PG (0.5 or 1 mmol), 1 ml of solvent and 3 mg of catalyst. Aliquots of the reaction mixture were withdrawn periodically by a syringe through a septum and analyzed by GC (Chromatec Crystal 5000.1, flame ionization detector, 30 m × 0.22 mm × 0.5 µm ZB-WAX capillary column, chlorobenzene as internal standard), GC-MC (Agilent 7000B system with triple-quadrupole mass-selective detector Agilent 7000 and GC Agilent 7890B, 30 m × 0.25 mm × 0.25 µm ZB-WAX capillary column), and HPLC (Agilent 1220 instrument, ZORBAX Eclipse Plus C18 Analytical 4.6 × 150 mm 5-µm column). Methyl glyoxal was determined as *ortho*-phenylenediamine derivative by GC [39]. Each experiment was reproduced 3–4 times. NMR spectra were collected using Bruker Avance-400 spectrometer (400.13 MHz).

In recycling experiments, the catalyst was filtered off after the reaction, washed with acetonitrile, dried at room temperature overnight, and then reused. The amount of chromium in filtrates was determined by inductively coupled plasma atomic emission spectroscopy (Agilent 4100 microwave spectrometer). After catalysis, Cr-MIL-101 was characterized by XRD, FT-IR and DTA/TGA (NETZSH STA 449F1 Jupiter coupled mass-spectrometer QMS 403D Aeolos, heating 10 K/min from 25 to 400 °C, Ar, Al₂O₃ crucible).

2.4. Adsorption measurements

All adsorption measurements were carried out at room temperature (25 °C). A concentrated (3.3 M) solution of an organic compound (PG, HA, MeOH or AcOH) was added by portions (30 µl)

Table 1

PG oxidation with TBHP over Cr-containing catalysts.

Catalyst	Conversion, % Product yield, ^a %					HA selectivity, %	
	PG	TBHP	HA	AAc	AA	on PG	on TBHP
Cr-MIL-101	10	65	8.8	1.0	0.2	88	53
Cr-MIL-100	11	4	7.6	1.0	0.1	69	>100 ^b
Cr ₃ (Ac) ₇ (OH) ₂	20	87	11.4	3.7	0.5	57 (69) ^c	52
No catalyst	3	~0	2.1	0.1	traces	70	n.d. ^d

Reaction conditions: 1 mmol PG, 0.25 mmol TBHP, 1 ml MeCN, PG/Cr = 76 (mol/mol), 50 °C, 7 h for MIL-101, MIL-100 and blank experiment and 5 h for Cr₃(Ac)₇(OH)₂ (time when PG conversion and HA yield reached their maximum values).

^a GC yield based on starting PG. Other identified products were formic acid, formaldehyde and acetone.

^b >100% selectivity formally calculated based on TBHP is due to a significant role of O₂ in the oxidation process.

^c In parentheses, at 10% PG conversion.

^d Not determined.

to a solution containing 2 ml of CH₃CN, 8 µl of *n*-octane (internal standard) and 20 mg of activated Cr-MIL-101(100). After the addition of each portion, the mixture was stirred for 5 min (this time is enough to reach the adsorption equilibrium [36]) and then MOF was separated by centrifugation (6000 rpm, 15 min) and the concentration of PG (HA, MeOH or AcOH) was determined by GC (3–5 measurements) using a gas chromatograph Chromos GC-1000 equipped with a flame ionization detector and a quartz capillary column BPX5 (30 m × 0.25 mm). Parallel, blank experiments (without MOF) were performed. The amount of adsorbed PG (HA, MeOH or AcOH) was determined as a difference between concentrations of the organic compound in the solutions with and without MOF multiplied on the solution volume. Adsorption constants were estimated using Langmuir (PG and HA) or Fowler (methanol) adsorption model.

3. Results and discussion

3.1. Comparison of the catalytic and adsorption behavior of Cr-MIL-100 and Cr-MIL-101

To suppress overoxidation processes, we evaluated the catalytic performance of Cr-MIL-100 and Cr-MIL-101 in PG oxidation under conditions of the oxidant deficiency ([PG]/[TBHP] = 1/0.25). Similar conditions were employed earlier for the TS-1/H₂O₂ system [19]. Table 1 presents the results on PG oxidation acquired over the Cr-MOFs in comparison with homogeneous chromium(III) acetate, Cr₃(CH₃COO)₇(OH)₂. In all cases, HA was the principle reaction product while the main byproducts were acetic acid (AAc) and acetaldehyde (AA) derived from C–C bond cleavage. Minor amounts of formic acid, formaldehyde and acetone were identified by GC-MS. While the former two products certainly originated from C–C cleavage, the latter could, in principle, be formed from PG via both oxidation [40] and acid-catalyzed [41] routes. Moreover, homolytic TBHP decomposition can also result in acetone formation [42]. Neither methyl glyoxal nor pyruvic acid, which might arise in the course of HA overoxidation, was found among the reaction products. The oxidation of the primary hydroxyl group of PG leading to lactaldehyde and lactic acid did not take place either. Note that PG conversion did not exceed 3% in the absence of any catalyst (see Table 1).

The corresponding kinetic curves for PG consumption and accumulation of the main products over the MOFs and homogeneous Cr(III) catalyst are given in Fig. 1. Although homogeneous Cr(III) acetate was more active than both Cr-MOFs and led to higher PG conversion (20% versus 10–11% with MOFs), it gave increased amounts of the C–C cleavage products, thereby resulting in lower HA selectivity. Even at a similar level of PG conversion (ca. 10%),

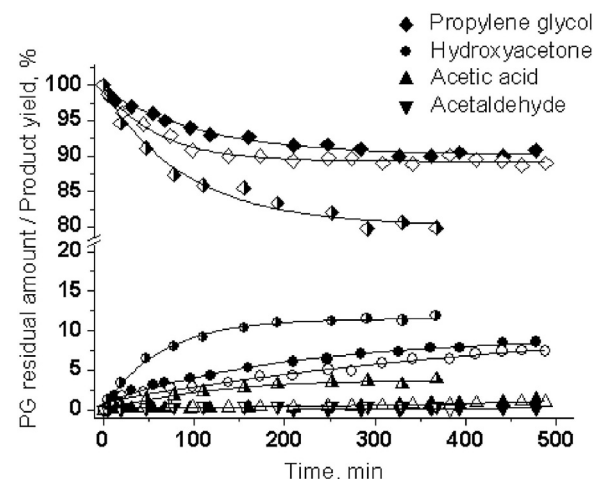


Fig. 1. PG oxidation with TBHP over Cr-containing catalysts: Cr-MIL-101—filled, Cr-MIL-100—open, and Cr₃(Ac)₇(OH)₂—half open symbols. Reaction conditions as in Table 1.

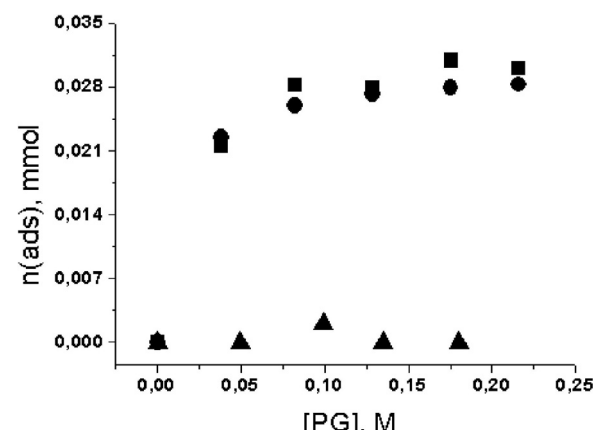


Fig. 2. Adsorption of PG from MeCN solution on Cr-MIL-100 (■), its fitting with Langmuir model (●), and adsorption of PG on Cr-MIL-101 (▲).

selectivity for HA was higher for MIL-101 (88% versus 69% for Cr(III) acetate). As one can see from Fig. 1, the initial rate of PG consumption over MIL-100 was higher than over MIL-101. The attainable level of substrate conversion was similar for both MOFs, but MIL-101 was more selective toward HA formation. The reaction stopped completely after 6–7 h although the oxidant consumption was not complete (see data in Table 1).

The oxidant utilization efficiency, i.e. HA selectivity based on TBHP consumed, was similar for MIL-101 and Cr(III) acetate and attained 52–53%. In this respect, the catalytic performance of MIL-100 was different: a very low conversion of TBHP was observed in the presence of this MOF and PG (see Table 1), leading formally to >100% HA selectivity based on TBHP. This indicates that TBHP was not the sole oxidant in the system and molecular oxygen contributed significantly into the oxidation process (*vide infra*).

To rationalize the different catalytic performance of MIL-100 and MIL-101, we investigated adsorption of PG on these MOFs. The corresponding adsorption isotherms are shown in Fig. 2. Surprisingly, only MIL-100 adsorbs PG from acetonitrile solution while MIL-101 does not. As one can judge from Fig. 2, Langmuir model provides a fairly good description of the experimental isotherm for MIL-100 ($K_{\text{ads}} = 80 \pm 23 \text{ M}^{-1}$ at 25 °C). The reasons for the different adsorption behavior of MIL-100 and MIL-101 are not yet completely clear. The structure of the primary chromium trimers and the mode of the arrangement of super tetrahedra (MTN struc-

Table 2

Effect of solvent nature on PG oxidation with TBHP over MIL-101.

Solvent	Time, ^a h	Conversion, %	Product yield, ^b %		
			HA	AAc	AA
CH ₃ CN	7	10	8.8	1.0	0.2
CH ₃ COOC ₂ H ₅	5.5	14	7.2	4.5	0.8
CH ₃ OH	2	5	3.1	0.3	traces
H ₂ O	7	8	1.6	3.0	0.3
CH ₃ CN ^c	7	9	7.5	1.1	0.1
CH ₃ CN/H ₂ O ^d	7	9	7.2	1.2	0.1
CH ₃ CN/H ₂ O ^e	7	8	1.6	1.5	0.2

Reaction conditions: 1 mmol PG, 0.25 mmol TBHP, 1 ml solvent, 3 mg Cr-MIL-101, 50 °C.

^a Time when PG conversion and HA yield reached their maximum values.

^b GC yield based on starting PG.

^c TBHP was used as 70% aqueous solution (0.5 M H₂O in the reaction mixture).

^d 3.9 M H₂O in CH₃CN.

^e MeCN/H₂O 1:1 vol/vol.

ture) are the same for both MIL-100 and MIL-101, but the specific linker affects the structure and size of the super tetrahedron. This results in the different geometrical parameters of the MOF structure, which in turn, might be responsible for the different affinity toward PG molecules (or their associates [43]). In contrast to PG, no adsorption of HA from acetonitrile was found on both MIL-100 and MIL-101 at 25 °C. Yet, no adsorption of acetic acid was established. These facts allowed us to suggest that neither adsorption of the principal oxidation product (HA) nor adsorption of the main detected by-product (AcOH) can be responsible for the catalyst deactivation.

On the other hand, a significant adsorption of methanol from MeCN was detected for Cr-MIL-101. The corresponding isotherm (Fig. S3 in SI) has an S-type shape, which is typical of Fowler model. This may indicate that, with increasing coverage of MIL-101 surface with methanol, its adsorption becomes easier, most likely, due to formation of hydrogen bonds between methanol molecules in the adsorbed layer. The consequences of the adsorption peculiarities for the catalytic performance of the MOFs will be discussed in the following sections.

3.2. Effect of solvent nature

Given that higher selectivity toward HA was attained over Cr-MIL-101, this MOF was preferably used in further experiments. Three organic solvents, acetonitrile, ethyl acetate and methanol, as well as water were used to evaluate the effect of solvent nature on PG oxidation over Cr-MIL-101. The results are presented in Table 2. The highest conversion of PG (14%) was attained in ethyl acetate. However, larger amounts of the C–C bond cleavage products formed in this solvent, resulting in lower selectivity for HA. In methanol, the reaction stopped after 2 h and PG conversion did not exceed 5%. A possible reason for that could be strong adsorption of methanol on Cr-MIL-101. Indeed, we found that this phenomenon does take place (see Fig. S3). Consequently, when methanol is used as solvent, its adsorption may prevent interaction of PG or TBHP with the catalyst surface. At the same time, methanol can act as inhibitor in radical chain processes.

The reaction took place in water and attained 8% conversion after 7 h, but HA selectivity and total carbon mass balance were poor. Acetic acid predominated among the identified products (see Table 2). We may suggest that the presence of water facilitates C–C bond cleavage and formation of unidentified condensation products. Importantly, the structure of MIL-101 remained intact after the reaction in water, as evidenced by XRD and FT-IR techniques (Figs. S4 and S5, respectively, in SI). On the other hand, use of aqueous solution of TBHP instead of anhydrous one (in this case the

Table 3

Effect of PG/TBHP molar ratio on PG oxidation over Cr-MIL-101.

[TBHP], M	Conversion, %			Yield on PG, ^a %		HA selectivity, %	
	PG	TBHP	HA	AAc	AA	on PG	on TBHP
0.125	7	86	6.0	0.8	0.05	86	57
0.25	10	65	8.8	1.0	0.2	88	53
0.5	12	48	8.2	1.2	0.4	68	34
0.25 ^b	11	26	9.3	1.3	0.3	85	>100

Reaction conditions: 1 mmol PG, 1 ml MeCN, 3 mg Cr-MIL-101, 50 °C, 7 h.

^a GC yield based on starting PG.

^b 6 mg Cr-MIL-101.

concentration of water in the system was 0.5 M) produced insignificant increase in the yield of C–C cleavage products (Table 2). The augmentation of water concentration up to 3.9 M resulted in only slight reduction of PG conversion and HA yield, indicating that relatively small amounts of water are not detrimental for the title reaction. On the other hand, large amounts of water in MeCN (1:1 vol/vol) led to a drastic decrease of HA yield, increase of AcOH yield and general deterioration of the carbon mass balance (see Table 2).

3.3. Effect of PG/TBHP molar ratio

To verify the effect of PG to TBHP molar ratio on the PG oxidation over MIL-101, the oxidant concentration in the reaction mixture was varied. The results are shown in Table 3. Selectivity for HA based on both PG and TBHP remained quasi constant in the range of 0.125–0.25 M of the oxidant but then it tended to decrease, most likely because HA overoxidation became significant. This was confirmed by the experiment where HA was used as the substrate instead of PG. In this case, acetic acid and acetaldehyde were the main products which formed with the yields of 8 and 1.4%, respectively, at HA conversion of 11% after the characteristic time of 7 h. Like in the oxidation of PG, no methyl glyoxal was found in the reaction mixture.

Although TBHP in all cases was used in deficiency relative to PG, its conversion did not reach 100% and decreased with increasing initial hydroperoxide concentration. In turn, PG conversion did not exceed 56% relative to the theoretical value that could be achieved if TBHP were completely used for PG oxidation. Since the adsorption study showed that no evident adsorption of HA occurs on the MOFs from MeCN solution (Fig. 2), we could assume that the incomplete conversion of the reagents might be caused by strong adsorption of by-products, for example, carboxylic acids. However, the adsorption study showed that no significant adsorption of AcOH takes place on MIL-101 from MeCN solution. Moreover, additives of AcOH into the reaction mixture produced no rate-retarding effects. On the contrary, additives of formic acid led to decreasing the reaction rate and attainable level of PG conversion (Fig. S6 in SI). Consequently, adsorption of HCOOH on Cr-MIL-101 can be responsible for the observed catalyst deactivation. The DTA/TGA data coupled with mass-spectrometry acquired for the sample of MIL-101 separated after the oxidation reaction corroborated desorption of formic acid together with formaldehyde and acetaldehyde.

3.4. Effect of reaction atmosphere and radical scavengers

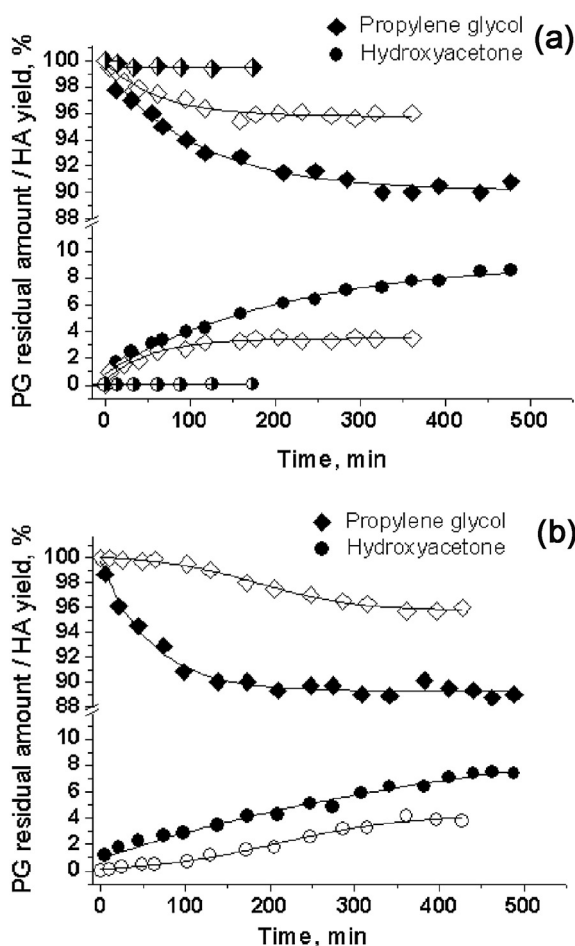
The presence of molecular oxygen can be essential for oxidative transformations over MOFs when TBHP is used as oxidant [33]. Indeed, involvement of O₂ in the PG oxidation process was unambiguously indicated by the >100% selectivity based on TBHP that had been achieved over MIL-100 (see Table 1). Participation of molecular oxygen in the PG oxidation was further confirmed by experiments carried out under inert atmosphere using MIL-101

Table 4

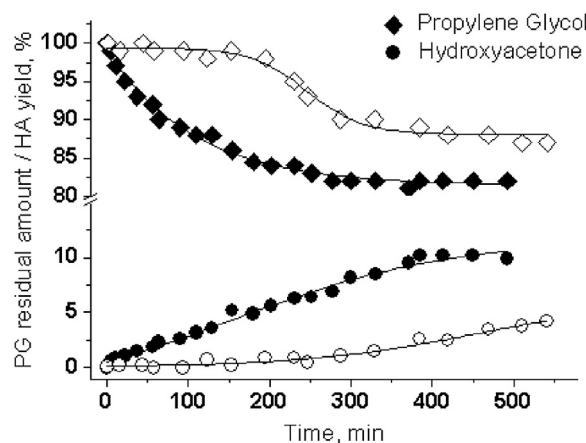
Effect of reaction atmosphere on PG oxidation over Cr-MIL-101.

Atmosphere	Conversion, %		Yield on PG, ^a %			HA selectivity, %	
	PG	TBHP	HA	AAc	AA	on PG	on TBHP
Air	10	65	8.8	1	0.2	88 (77) ^b	53
Ar	4	15	3.5	0.3	0.05	88	93
Air ^c	~0.5	n.d. ^d	traces	traces	traces	n.d.	n.d.
Air ^e	3	n.d.	2.3	0.2	traces	77	n.d.

Reaction conditions: 1 mmol PG, 0.25 mmol TBHP (if any), 1 ml MeCN, 3 mg Cr-MIL-101, 50 °C, 7 h.

^a GC yield based on starting PG.^b In parentheses, at 4% PG conversion.^c No TBHP was added.^d Not determined.^e 0.05 mmol TBHP.**Fig. 3.** PG oxidation with TBHP over MIL-101 (a) and MIL-100 (b) in air (filled symbols) and under Ar (open symbols). In (a) half-open symbols correspond to reaction in air without TBHP.

and MIL-100. The results of these experiments are presented in Table 4 (MIL-101) and Fig. 3 (MIL-101 in comparison with MIL-100). Both substrate and TBHP conversions differed significantly from the experiment under air. The difference in the initial reaction rates under Ar and air was more pronounced for MIL-100 than for MIL-101 (compare kinetic curves in Fig. 3a and b). Furthermore, the reaction in inert atmosphere over MIL-100 revealed an induction period while no induction period was observed in air (see Fig. 1). These results agree with the low TBHP conversion observed over MIL-100 in the presence of PG (see Table 1). Previously, we found that MIL-100 and MIL-101 are active in TBHP decomposition in chlorobenzene in the absence of any oxidizable organic substrate,

**Fig. 4.** PG oxidation over Cr-MIL-101 with (open) and without (filled symbols) additives of ionol (6.6 μmol). Reaction conditions: 0.5 mmol PG, 0.125 mmol TBHP, 3 mg Cr-MIL-101, 1 ml MeCN.

the rate of decomposition being just somewhat higher for MIL-101 [38]. In this work, we also measured the rate of TBHP decomposition in MeCN in the absence of PG and found a similar activity for both MIL-100 and MIL-101. Therefore, we may tentatively assume that the pronounced adsorption of PG on MIL-100 depicted in Fig. 2 disfavors adsorption of TBHP and blocks its access to the active Cr centers, which suppresses TBHP activation through its decomposition and enhances the contribution of molecular oxygen into the overall oxidation rate over MIL-100.

The product distribution under argon was close to that realized in air, indicating that the oxidation mechanism does not change drastically in the absence of molecular oxygen. Dissimilar to what has recently been observed for aerobic indene oxidation [44], no reaction occurred in the absence of TBHP. Moreover, if we introduced small additives of TBHP (0.05 mmol) into the reaction, conversion of PG in this case did not exceed 3% over both MIL-100 and MIL-101 (for the latter, see data in Table 4), which might indicate a more complicated role of TBHP than to be a simple initiator.

Additives of the conventional radical chain scavenger, ionol, produced a strong rate-retarding effect (Fig. 4). Coupled with the disclosed role of molecular oxygen, this strongly supports radical chain mechanism for PG oxidation over MIL-101 and MIL-100. According to the results of the adsorption experiment (Fig. 2), no PG adsorption occurs on Cr-MIL-101 from MeCN, which excludes activation of the substrate molecule on the active sites of the catalyst. All these facts collectively allowed us to suggest that PG oxidation, at least over MIL-101, involves TBHP homolytic decomposition on Cr(III) centers, giving rise to radicals which further react with substrate molecules through preferable abstraction of H atom bound to C2 atom.

3.5. Effect of temperature and nature of catalysis

The title reaction is very slow at room temperature (only 2% PG conversion after 7 h). The increase in the reaction temperature from 40 to 70 °C accelerated the reaction and increased the attainable PG conversion; however, it had very little effect on the product selectivity. The initial rate of PG oxidation exhibited a typical Arrhenius dependence (Fig. 5). The activation energy (E_a) estimated from the corresponding plot equals to 67 kJ/mol. Such value is typical for reactions controlled by chemical interaction, because for reactions that are controlled by diffusion of reactants, the value of E_a is typically below 17 kJ/mol [45]. It is noteworthy that similar E_a (63 kJ/mol) was previously found for anthracene oxidation with TBHP over Cr-MIL-100 and Cr-MIL-101, where interaction between

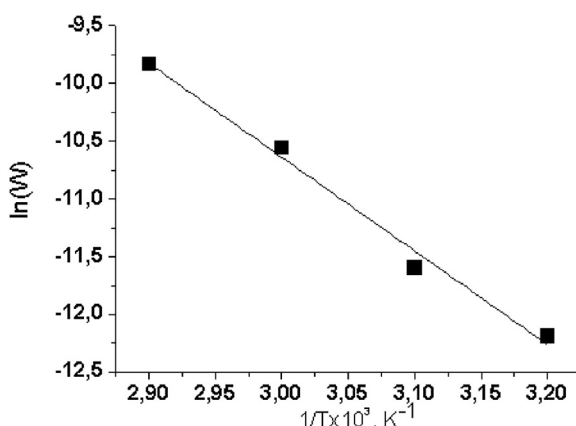


Fig. 5. Arrhenius plot for PG oxidation with TBHP over MIL-101.

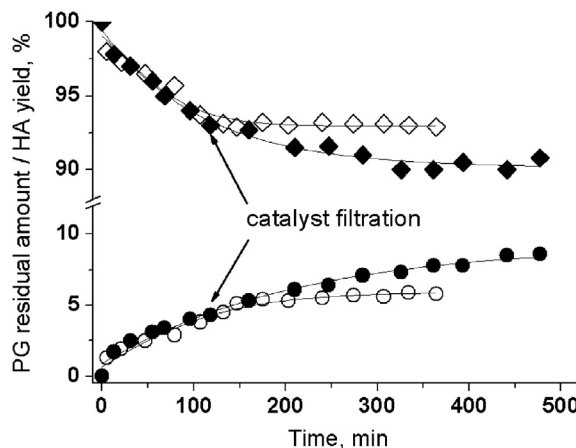


Fig. 6. Hot catalyst filtration test at 50 °C. Filled and open symbols correspond to kinetic curves acquired without and with catalyst separation, respectively.

TBHP and Cr(III) centers within the MOF framework to produce an active oxidizing species was suggested as the rate-limiting step [38]. This fact coupled with the results of the adsorption experiments that had been discussed in Section 3.1 allowed us to make an assumption that activation of TBHP may also determine the rate of the overall oxidation process. Further kinetic studies would be useful to verify this hypothesis.

Previously, some of us demonstrated that reaction temperature may strongly affect the nature of catalysis over MOFs [36]. Indeed, we found that the PG oxidation proceeded with the same rate after catalyst removal by hot filtration at 70 °C. The amount chromium in the filtrate determined by atomic emission spectroscopy was 34 ppm, indicating substantial leaching of active Cr species under the reaction conditions. After catalyst separation at 60 °C, the reaction did not stop completely in the filtrate but it continued with a lower rate, although the chromium amount in the filtrate did not exceed 0.1 ppm. At the same time, a blank, catalyst-free experiment at 60 °C revealed some PG oxidation to HA under the conditions employed. Hence, the observed continuation of the reaction after catalyst filtration at 60 °C may be caused by thermal activation of the oxidant. A similar conclusion was drawn for tetralin oxidation with TBHP over MIL-101 [34]. In contrast, the hot catalyst filtration test performed at 50 °C (Fig. 6) showed that both PG consumption and HA accumulation stopped completely after separation of the catalyst, which confirmed the truly heterogeneous nature of the catalysis over Cr-MIL-101 at this temperature. Again, the amount of chromium in the filtrate did not exceed 0.1 ppm. For this reason,

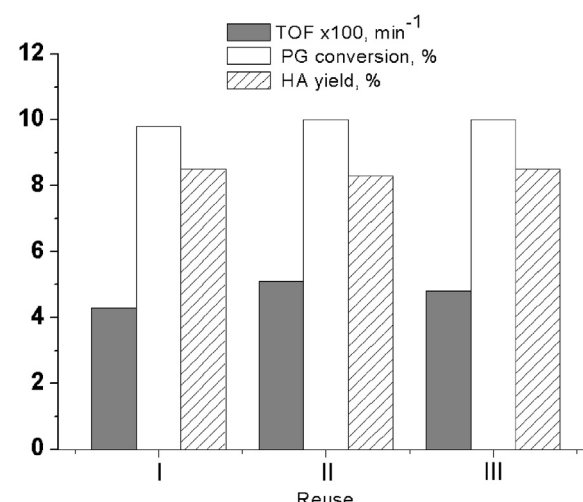


Fig. 7. Recycling of Cr-MIL-101 in PG oxidation with TBHP. Reaction conditions as in Table 1.

all the catalytic studies presented in this work (Tables 1–4 were carried out at 50 °C).

3.6. Catalyst stability and reusability

Cr-MIL-101 features fairly good thermal [28] and hydrothermal [46] stability and can act as a truly heterogeneous catalyst under oxidative conditions at elevated temperatures [31–38]. However, the polarity of substrate and products as well as their concentrations and the reaction temperature can be critical for the catalyst stability. As was mentioned above leached chromium species (34 ppm) were found in the filtrate during PG oxidation at 70 °C and significant contribution of homogeneous catalysis was established in this case by the hot filtration test. For this reason, we carried out recycling experiments at 50 °C, under the conditions of the truly heterogeneous catalysis. As one can judge from Fig. 7, the MIL-101 catalyst could be recycled, at least 3 times, without loss of the catalytic activity and selectivity. It is noteworthy that no catalyst reactivation was needed before reuse. The catalyst was simply separated by filtration after PG conversion reached its maximum value (ca. 10%), then washed, dried in air and used in the next run with a new portion of the reagents. The retention of the MIL-101 structure was confirmed by FT-IR and XRD techniques. The XRD patterns of the catalyst before and after three operation cycles are shown in Fig. 8 while Fig. S2 in the SI presents the corresponding IR spectra.

4. Conclusions

In this work, we demonstrated that the chromium-based metal-organic frameworks MIL-101 and MIL-100 are able to catalyze selectively oxidation of propylene glycol using TBHP as oxidant. The reaction proceeds with high regioselectivity for the secondary alcohol group. No oxidation of the primary hydroxyl group of PG leading to lactaldehyde and lactic acid occurs. Selectivity toward hydroxyacetone attains 88% at ca. 10% PG conversion with MIL-101 as catalyst and acetonitrile as solvent; the oxidant utilization efficiency is 53–57%. Water facilitates C–C bond cleavage processes. With homogeneous chromium acetate, PG conversion can reach 20% under similar reaction conditions, but selectivity for HA was lower than with MIL-101 during the overall course of the reaction. The pronounced impacts of radical chain scavengers and molecular oxygen on the reaction rate suggest radical chain mechanism of the oxidation process. The adsorption study revealed that MIL-101

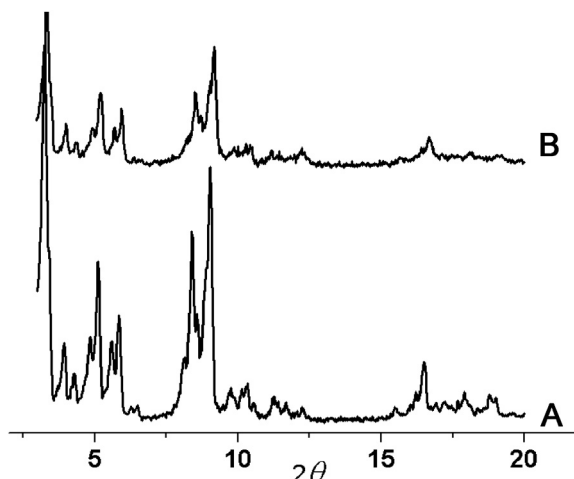


Fig. 8. XRD patterns of MIL-101 before and after 3 catalytic runs (reaction conditions as in Table 1).

and MIL-100 possess different affinity toward PG, and this has consequences for their catalytic performances. The strong adsorption of PG on MIL-100, most likely, hinders adsorption of the oxidant, TBHP, on the chromium active centers. The nature of catalysis depends on the reaction temperature. At 50 °C, the nature of the catalysis over MIL-101 is truly heterogeneous and no metal leaching into solution occurs. The MIL-101 catalyst can be recycled with maintenance of the catalytic performance and the MOF structure during, at least, three operation cycles.

Acknowledgements

The authors thank Dr. K. A. Kovalenko for the synthesis of MIL-100 and Dr. A. N. Shmakov and V. A. Utkin for XRD and GC-MS measurements, respectively. The research was supported by “The Tomsk State University Academic D.I. Mendeleev Fund Program” grant (8.2.07.2015) in 2015–2016 and partially (I.D.I., I.Y.S. and O.A.K.) supported by the Russian Foundation for Basic Research (grant No. 13-03-00413).

Appendix A. Supplementary data

Supplementary data associated with this article can be found, in the online version, at <http://dx.doi.org/10.1016/j.cattod.2016.04.008>.

References

- [1] R.A. Sheldon, J.K. Kochi, *Metal-Catalyzed Oxidations of Organic Compounds*, Academic Press, New York, 1981.
- [2] G. Cainelli, G. Cardillo, *Chromium Oxidations in Organic Chemistry*, Springer, Berlin, 1984.
- [3] G. Tojo, M. Fernández, *Oxidation of Alcohols to Aldehydes and Ketones*, Springer, New York, 2006.
- [4] R. Sheldon, I.W.C.E. Arends, U. Hanefeld, *Green Chemistry and Catalysis*, Wiley-VCH, Weinheim, 2007.
- [5] Fine Chemicals through Heterogeneous Catalysis, in: R.A. Sheldon, H. van Bekkum (Eds.), Wiley-VCH, Weinheim, 2001.
- [6] Liquid Phase Oxidation via Heterogeneous Catalysis: Organic Synthesis and Industrial Applications, in: M.G. Clerici, O.A. Kholdeeva (Eds.), Wiley, New Jersey, 2013.
- [7] P.Y. Dapens, C. Mondelli, Renez-Ramirez, *J. Chem. Soc. Rev.* 44 (2015) 7025–7043.
- [8] G. Knothe, J. Krahl, J.V. Gerpen, *The Biodiesel Handbook*, AOCS, Champaign, 2005.
- [9] M. Ai, K. Ohdan, *J. Mol. Catal.* 159 (2000) 19–24.
- [10] M. Ai, A. Motohashi, S. Abe, *Appl. Catal. A: Gen.* 246 (2003) 97–102.
- [11] S. Sato, R. Takahashi, T. Sodesawa, H. Fukuda, T. Sekine, E. Tsukuda, *Catal. Commun.* 6 (2005) 607–610.
- [12] J. Shen, W. Shan, Y. Zhang, J. Du, H. Xu, K. Fan, W. Shen, Y. Tang, *J. Catal.* 237 (2006) 94–101.
- [13] J. Shen, W. Shan, Y. Zhang, J. Du, H. Xu, K. Fan, W. Shen, Y. Tang, *Chem. Commun.* (2004) 2880–2881.
- [14] L. Prati, M. Rossi, *J. Catal.* 176 (1998) 552–560.
- [15] N. Dimitratos, J.A. Lopez-Sanchez, S. Meenakshisundaram, J.M. Anthonykutty, G. Brett, A.F. Carley, S.H. Taylor, D.W. Knight, G.J. Hutchings, *Green Chem.* 11 (2009) 1209–1216.
- [16] M.B. Griffin, A.A. Rodriguez, M.M. Montemore, G.R. Monnier, Ch. T. Williams, J.W. Meldin, *J. Catal.* 307 (2013) 111–120.
- [17] Y. Ryabenkova, Q. He, P.J. Miedziak, N.F. Dummer, S.H. Taylor, A.F. Carley, D.J. Morgan, N. Dimitratos, D.J. Wilcock, D. Bethell, D.W. Knight, D. Chadwick, Ch. Kiely, G.J. Hutchings, *Catal. Today* 203 (2013) 139–145.
- [18] M. Besson, P. Gallezot, C. Pinel, *Chem. Rev.* 114 (2014) 1827–1870.
- [19] R.A. Sheldon, J. Dakka, Erdöl Erdgas Kohle 109 (1993) 520–522.
- [20] O.A. Kholdeeva, B.G. Donoeva, T.A. Trubitsina, G. Al-Kadamany, U. Kortz, *Eur. J. Inorg. Chem.* 34 (2009) 5134–5141.
- [21] N.H. Mohamad, R. Awang, W.M.Z.W. Yunus, *Am. J. Appl. Sci.* 8 (2011) 1135–1139.
- [22] J. Long, O. Yaghī, *Chem. Soc. Rev.* 38 (2009) 1257–1283.
- [23] Functional metal-organic frameworks: gas storage, separation and catalysis, in: M. Schröder (Ed.), *Top. Curr. Chem.*, vol. 293, Springer, 2010.
- [24] Metal-Organic Frameworks: Applications from Catalysis to Gas Storage, in: D. Farrusseng (Ed.), Wiley, Weinheim, 2011.
- [25] Metal Organic Frameworks as Heterogeneous Catalysts, in: F. Llabrés i Xamena, J. Gascon (Eds.), RCS Publishing, 2013.
- [26] H.-C. Zhou, S. Kitagawa, *Chem. Soc. Rev.* 43 (2014) 5415–5418.
- [27] A. Corma, H. Garcia, F.X. Llabrés i Xamena, *Chem. Rev.* 110 (2010) 4606–4655.
- [28] G. Férey, C. Mellot-Draznieks, C. Serre, F. Millange, J. Dutour, S. Surble, I. Margioliaki, *Science* 309 (2005) 2040–2042.
- [29] G. Férey, C. Serre, C. Mellot-Draznieks, F. Millange, S. Surble, J.D.I. Margioliaki, *Angew. Chem.* 116 (2004) 6456–6461.
- [30] Y.K. Hwang, D.-Y. Hong, J.-S. Chang, H. Seo, M. Yoon, J. Kim, S.H. Jhung, C. Serre, G. Férey, *Appl. Catal. A: Gen.* 358 (2009) 249–253.
- [31] Y.K. Hwang, G. Férey, U.-H. Lee, J.-S. Chang, Liquid phase oxidation of organic compounds by metal-organic frameworks, in: M.G. Clerici, O.A. Kholdeeva (Eds.), *Liquid Phase Oxidation via Heterogeneous Catalysis: Organic Synthesis and Industrial Applications*, Wiley, New Jersey, 2013, pp. 371–410.
- [32] N.V. Maksimchuk, O.V. Zalomaeva, I.Y. Skoblev, K.A. Kovalenko, V.P. Fedin, O.A. Kholdeeva, *Proc. R. Soc. A* 468 (2012) 2017–2034.
- [33] N.V. Maksimchuk, K.A. Kovalenko, V.P. Fedin, O.A. Kholdeeva, *Chem. Commun.* 48 (2012) 6812–6814.
- [34] J. Kim, S. Bhattacharjee, K.-E. Jeong, S.-Y. Jeong, W.-S. Ahn, *Chem. Commun.* (2009) 3904–3906.
- [35] N.V. Maksimchuk, K.A. Kovalenko, M.S. Melgunov, V.P. Fedin, O.A. Kholdeeva, *Adv. Synth. Catal.* 352 (2010) 2943–2948.
- [36] I.Y. Skoblev, A.B. Sorokin, K.A. Kovalenko, V.P. Fedin, O.A. Kholdeeva, *J. Catal.* 298 (2013) 61–69.
- [37] O.A. Kholdeeva, I.Y. Skoblev, I.D. Ivanchikova, K.A. Kovalenko, V.P. Fedin, A.B. Sorokin, *Catal. Today* 238 (2014) 54–61.
- [38] I.D. Ivanchikova, I.Y. Skoblev, O.A. Kholdeeva, *J. Organomet. Chem.* 793 (2015) 175–181.
- [39] G.V. Mamontov, O.V. Magaev, A.S. Knyazev, O.V. Vodyankina, *Catal. Today* 203 (2013) 122–126.
- [40] E. Diaz, M.E. Sad, E. Iglesia, *ChemSusChem* 3 (2010) 1063–1070.
- [41] T.D. Courtney, V. Nikolakis, G. Mpourmpakis, J.G. Chen, D.G. Vlachos, *Appl. Catal. A: Gen.* 449 (2012) 59–68.
- [42] N.M. Emanuel, E.T. Denisov, Z.K. Maizus, *Liquid Phase Oxidation of Hydrocarbons*, Plenum, New York, 1967.
- [43] L.H. Thomas, R. Meatyard, *J. Chem. Soc. A: Inorg. Phys. Theor.* (1966) 92–96.
- [44] A. Santiago-Portillo, S. Navalón, F.G. Cirujano, F.X. Llabrés i Xamena, M. Alvaro, H. Garcia, *ACS Catal.* 5 (2015) 3216–3224.
- [45] P. Atkins, J. De Paula, *Elements of Physical Chemistry*, 6th ed., University Press, Oxford, 2013.
- [46] J.J. Low, A.I. Benin, P. Jakubczak, J.F. Abrahamian, S.A. Faheem, R.R. Willis, *J. Am. Chem. Soc.* 131 (2009) 15834–15842.